SolarPACES 2022, 28th International Conference on Concentrating Solar Power and Chemical Energy Systems
Solar Fuels and Chemical Commodities
https://doi.org/10.52825/solarpaces.v1i.748

Published: 02 Feb. 2024

Hydrogen Production via Off-Sun Solar-Thermal Supercritical Water Gasification and Membrane Reforming of Piggery Waste

Louise Bardwell[1][https://orcid.org/0000-0001-9933-4585], Alireza Rahbari[1][https://orcid.org/0000-0001-6363-739X], and John Pye[1][https://orcid.org/0000-0001-8026-0045]

[1] School of Engineering, Australian National University, Canberra, Australia

Abstract. Supercritical water gasification (SCWG) represents an emerging technology for liquid fuel synthesis, offering large potential in significantly improving the efficiency and environmental impact of clean fuel production. Compared to conventional gasification, SCWG proceeds at much lower temperatures, allowing char and tar-free gasification of biomass and for low-quality and high-moisture content biomass to be used. As the thermochemical processes involved in SCWG and steam methane reforming (SMR) are highly endothermic, combining them with concentrated solar power (CSP) and thermal energy storage (TES) could allow the process to be driven solely by renewable energy. As such, this work models an off-sun SCWG/SMR system using novel molten salt, proposed to reach up to 600°C [1], which overcomes the previously limiting molten salt temperature of 550°C. Using an off-sun configuration, it deals with the on-sun configuration's issues of degraded lifetime and creep-fatigue, allowing for uniform heating and a reduced load on the reactors. The novel technology of an integrated Pd-based membrane reactor, highly selective to H_2, was chosen given its ability to carry out SMR at temperatures in the viable range of new molten salts. The system uses a waste feedstock, piggery waste, to provide the dual benefit of reducing the environmental cost associated with piggery waste's release of CH_4. From the model created in Aspen Plus, a plant output of 7.2 kmolH_2/h (1,135 Nm³/h of H_2), was obtained with a flow rate of 150 kg/h of dry piggery waste, a membrane area of 131.8 m², and a 73% CH_4 conversion from the feed.

Keywords: Supercritical Water Gasification, Off-Sun, Membrane Reforming, Hydrogen, Solar Fuel

1. Introduction

Bioenergy, produced from the conversion of biomass, has been identified by the IPCC as a major contributor in all scenarios to achieving the Paris Agreement and limiting global warming to 1.5°C [2]. Specifically, bioenergy in the form of biofuels, including gaseous fuels like hydrogen and liquid fuels like biodiesel, biomethane, and bioethanol, has the potential to replace petroleum-based fuels and, when produced using renewable energy sources, can be carbon neutral [3]. Biofuels can bridge gaps in key sectors like industry and transport that cannot be met by renewable electrification, including heavy transport and high-heat industrial processes, and can help overcome the intermittency of solar and wind energy by providing an alternate means of energy storage.

Supercritical water gasification (SCWG) represents an emerging technology for such liquid fuel synthesis, offering significant potential for improvement to the efficiency and environmental impact of biofuel production [4]. Unlike traditional gasification, SCWG allows char and tar-free

gasification of biomass, and for low-quality and high-moisture content biomass to be used [5]. Producing a methane-rich biogas, SCWG can be coupled with downstream reforming processes like steam methane reforming (SMR) to produce syngas, a gas mixture of H_2 and CO, which can then be used in Fischer Tropsch (FT) synthesis to produce hydrocarbons like biodiesel and biomethanol [5]. As the thermochemical processes involved in SCWG are highly endothermic, often operated at temperatures above 550°C, the use of concentrated solar power (CSP) offers exciting potential for driving the SCWG reaction using renewable energy. Two main methods of CSP-driven SCWG have been identified in literature, referred to in this work as on-sun or off-sun. The on-sun method directly uses incoming concentrated solar radiation to run the SCWG reactors at temperatures around 750°C, while the off-sun method combines a CSP plant with thermal energy storage that acts as the heat transfer fluid (HTF) for the SCWG reaction at temperatures of around 550-600°C [1].

In previous work, Rahbari and Pye investigated a technology for converting farmed microalgae to solar fuels. In their initial work, they maximised the exergy efficiency of the SCWG process using a CSP thermal input [6], which then inspired the design and optimisation of a complete on-sun CSP-driven SCWG/SMR/FT system [7], [8]. Their final works reviewed the microalgae SCWG system, discussing the potential benefits of CSP integration [9], [10]. They found that the on-sun configuration of the system was limited due to the need for high-cost materials, thermal stresses, and mismatch between the fluctuating solar resource and steady thermal duty of the plant. The use of the off-sun configuration was therefore proposed by the authors to overcome these issues of degraded lifetime and creep-fatigue, allowing for uniform heating and a reduced load on the reactors. As conventional SMR requires temperatures of up to 850-950°C, the proposed off-sun configuration was however limited by the temperature bounds of thermal energy storage at 550-600°C, meaning it was incapable of meeting the high temperatures needed to drive the SMR reactions without additional thermal input.

The novel technology of an integrated Pd-based membrane reformer, highly selective to H_2, can overcome this limitation, allowing for SMR to be performed at temperatures in the viable range of new molten salts due to its continual removal of permeated H_2. Past projects, specifically the CoMETHy project [1], [11], have developed promising integrated membrane reformers, incorporating a high degree of compactness and flexibility to the type of feedstock used for the conversion. This flexibility allows the use of alternate feedstocks, including waste feedstocks like piggery waste. In agriculture, manure management is the third highest source of emissions [12], accounting for over two thirds of total emissions in pork production. Being the largest source of emissions associated with pork production, alternative solutions to pork effluent management focused on the capture and reuse of methane, therefore have the potential to significantly reduce emissions associated with the pork industry [13]. Using piggery waste as the feedstock in an off-sun SCWG/SMR system therefore can provide the additional benefit of reducing the environmental cost of piggery waste associated with its release of CH_4 and run-off into waterways.

The remainder of this paper is organised as follows: Section 2 provides a description of the model, including the CSP and molten salt storage system, SCWG reaction, membrane reformer, and selected piggery waste feedstock. Section 3 examines the results of the two reactor models, using sensitivity analysis to discuss the impact of key assumptions and design parameters. Section 4 concludes the paper.

2. Model Description

2.1. System Description

The proposed system comprises of two key reactors utilising 600°C solar salt supplied from a co-located CST plant as heat carriers: a SCWG reactor (MS-SCWG) that will convert the feedstock into biogas, and an integrated membrane reactor (MS-IMR) that will produce pure H_2

and CO_2 streams. The MS-SCWG reactor comprises of a shell and tube heat exchanger, with molten salt flowing in the shell and the wet feedstock flowing in the tubes. The design and performance for the MS-IMR was taken from that developed in the CoMETHy project [1], [11], but with molten salt flowing at 590°C rather than 540°C, and using the product biogas from the MS-SCWG reactor as the feed stream. The CST plant, storage, and reactors were sized at 2.3 MWth with 12-hour storage. To model the system, Aspen Plus V8.8 software was used (Figure 1), taking a Peng-Robinson Equation of State (PREoS) with van der Waals mixing rule for thermodynamic property calculations and a sequential modular simulation approach.

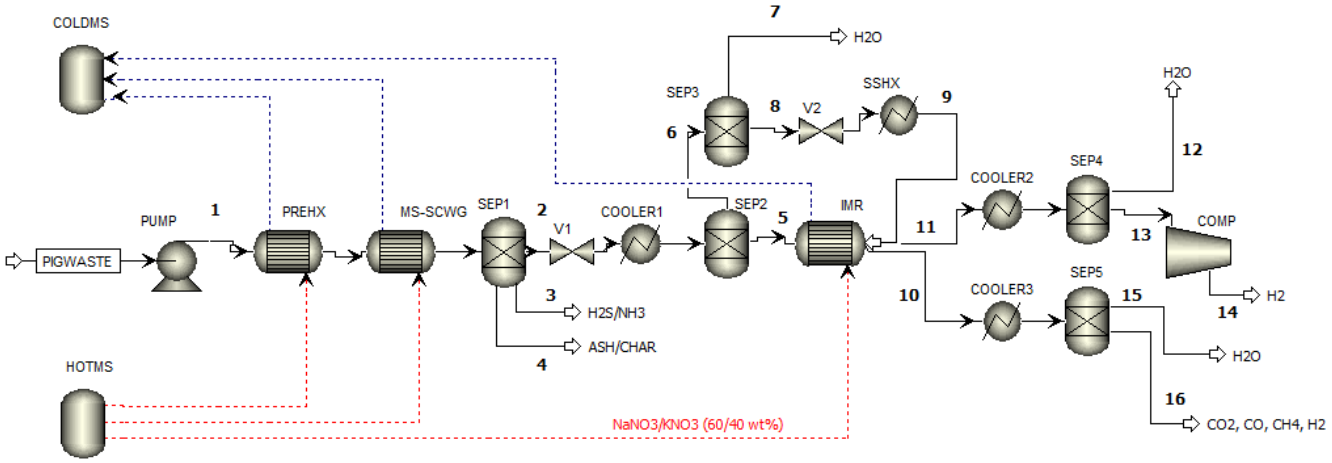

Figure 1. Simplified Aspen Plus flowsheet for system.

2.2. Piggery Waste Feedstock

Table 1. Ultimate and proximate analysis of piggery manure [14].

	Mass % (dry basis)
Proximate analysis	
Moisture content	0
Volatile matter	71.0
Fixed carbon	18.2
Ash content	10.9
Ultimate analysis	
Carbon	46.4
Hydrogen	6.9
Nitrogen	1.8
Sulphur	0.6
Oxygen	33.4
	Mass % (dry basis)
Proximate analysis	
Moisture content	0
Volatile matter	71.0
Fixed carbon	18.2
Ash content	10.9
Ultimate analysis	
Carbon	46.4
Hydrogen	6.9
Nitrogen	1.8
Sulphur	0.6
Oxygen	33.4

Piggery manure is composed of organic matter, nutrients, including nitrogen and phosphorus, salts, and microorganisms. It has a high moisture content, typically >75%, and therefore low wet mass methane potential, meaning it is inappropriate for traditional gasification without drying and has low performance in anaerobic digestion systems but is well suited to SCWG. The piggery waste was modelled using its ultimate and proximate analysis, which determine the mass concentrations of its major organic chemical elements, carbon, hydrogen, nitrogen, sulfur, and oxygen, and its mass percentages of moisture, volatile matter, fixed carbon, and ash content, respectively. The ultimate and proximate analysis used in this work has been summarised in Table 1.

2.3. CSP and Molten Salt Storage

Concentrating solar power (CSP) technology has seen significant advancements in the last few decades, with large-scale storage options being developed to offer viable means of overcoming the intermittency of solar energy supply associated with on-sun operation, and allowing the 24-hour operation of industrial procedures. CSP systems use a combination of mirrors or lenses to concentrate direct-beam solar radiation and produce useful forms of energy like heat, electricity, or fuels through various downstream technologies. One of the most common CSP systems commercially deployed is the central receiver tower configuration, where solar radiation is concentrated by factors of 500 to several thousand by a field of heliostats and intercepted by a receiver that converts it to thermal energy. This thermal energy can either be directly used to drive chemical reactions, converted to electricity via thermal power cycles, or carried away via a HTF.

One of the most promising storage options that has been developed is two-tank molten salt storage, wherein molten salts act as both the HTF and heat storage fluid (HSF). In the two-tank approach, the molten salt is cycled between a hot tank (~565°C) and a cold tank (~290°C) [15]. Molten salts have the benefit of high boiling points, low viscosity, low vapour pressure, high volumetric heat capacities, and therefore low operating costs. Currently, hot tank molten salt storage has achieved temperatures of up to 565°C, with future technologies offering the potential to reach up to 600°C [1]. Known as “solar salt”, $NaNO_3/KNO_3$ (60/40 w/w) has emerged as the most promising molten salt for solar applications.

For this model, a central receiver tower configuration with two-tank storage was selected. The off-sun system, consisting of a series of shell and tube heat exchangers where the molten salt flows in the shell at temperatures up to 600°C and feedstock flows in the tubes under high pressure, allows the following benefits:

- fixes mismatch between fluctuating solar resource and steady thermal duty profile of chemical plant, and
- reduces the need for high performance alloys and resolves issues of degraded lifetime and creep fatigue due to lower thermal stresses, lower peak temperatures, and more continuous operation.

2.4. Supercritical Water Gasification (SCWG)

Traditional gasification technologies encounter several difficulties that limit their development and application. Firstly, the quality of the product gas is often low due to contamination by impurities like char and tar [16]. Secondly, standard gasification technologies require dry biomass, as a high percentage of moisture in the biomass will decrease the temperature inside the gasifier, reducing its efficiency. As biomass usually contain a high percentage of moisture this then requires that biomass be dried before it is fed into the gasifier, contributing substantial energy and cost additions to the process.

The use of supercritical water in the process of supercritical water gasification (SCWG) has therefore emerged as a potential solution to these limitations of typical gasification. For

pure water, the critical point is 374°C and 22.1 MPa, meaning above this temperature and pressure, water is in its supercritical phase. In this supercritical phase, the physical properties of water change drastically, with water behaving as a homogeneous fluid phase exhibiting both liquid-like density and gas-like viscosity [10]. In the supercritical state, water's density is reduced by an order of magnitude, drastically reducing its hydrogen bonding and the dipole-dipole interaction and allowing water to act as a non-polar rather than polar solvent with a high solubility for organics and low solubility for salts. This unique solvent property, opposite to that experienced in normal conditions, allows char and tar-free gasification of biomass, and the potential for low-quality and high-moisture content biomass to be converted into gas [17].

2.5. Membrane Reformer

Palladium has emerged as the leading dense metal membrane due to its high selectivity to hydrogen. Pd and Pd-based membranes can dissociate molecular hydrogen into monatomic form ready for its fast diffusion through its lattice. Pd alone however is expensive and so it is often alloyed with inexpensive elements like Cu, with alloys like Pd-Ag having almost double the hydrogen permeability of pure Pd [18].

The performance of Pd-based membrane reactors can be described by the reaction's conversion, permeate flow rate, hydrogen yield, and hydrogen recovery. The H_2 permeation through a Pd-based membrane is usually described by Sieverts' law,

$$J_{H_2} = P_{H_2}\left(\sqrt{P_{ret}} - \sqrt{P_{perm}}\right) \quad (1)$$

where P_{H_2}, P_{ret}, and P_{perm} refer to the membrane's permeance, hydrogen partial pressure on the retentate side, and hydrogen partial pressure on the permeate side, respectively. Pd-based membrane reformers benefit from a high selectivity, but, as with other membranes, face challenges regarding degradation and stability over time, as well as potentially higher costs.

Of the membrane reactor configurations, including packed bed and fluidised bed configurations, few have been designed to operate with renewable energy vectors like off-sun CSP. The CoMETHy project therefore stands as the key reference point for an off-sun membrane reactor. Running from December 2011 to December 2015, the CoMETHy (Compact Multifuel-Energy to Hydrogen converter) project led to the development of an innovative, compact membrane reformer, in which the membrane is integrated with the catalyst bed and the molten salts heat exchanger. The integrated membrane reformer (IMR) achieved an experimental production rate of up to 3 Nm^3/h of pure, permeated hydrogen (>99.8% H_2 with < 100 ppm CO content) and methane conversions of over 60%, which are over double that attainable in a conventional reformer under the same low temperature conditions. From characterisation of the membrane, a H_2 permeance of 10-15 $(Nm^3/h)/m^2/bar^{0.5}$ was obtained. In a TEA performed for the membrane reactor, the pilot membrane reactor was then scaled up to a 1500 Nm^3/h capacity, taking the hydrogen permeance of 15 $(Nm^3/h)/m^2/bar^{0.5}$, a methane conversion of 73%, and hydrogen recovery of 90%. A sweep steam, designed to achieve a steam-to-carbon ratio of 3.2 (on molar base), was injected in the inner tube of the membrane reactor to increase the difference of the hydrogen partial pressures between the feed and permeate sides of the reactor by removing permeated hydrogen from the reactor. The results of this IMR design were used in this work's model, with Figure 2 showing the 2D representation for the IMR that was implemented.

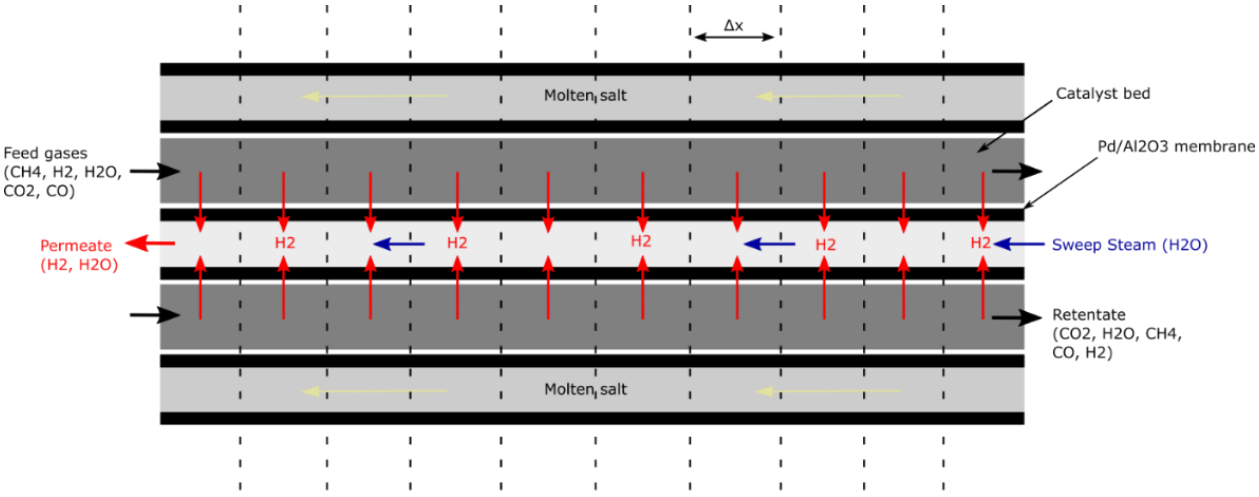

Figure 2. Diagram of 2D MS-IMR model used for sequential modular simulation.

3. Results and Discussion

3.1. SCWG Reactor

In the SCWG reactor, it was assumed all ash and 15% of the char do not interact in the MS-SCWG equilibrium reactions and can be removed, and that all nitrogen (N_2) and sulfur (S) react to form NH_3 and H_2S that is then removed from the MS-SCWG products stream. The piggery waste enters the system at standard conditions of 25°C and 1 bar pressure. The piggery waste is first sent to a pump where it is pressurised to 240 bar pressure. It is then sent through a series of heaters where it is heated to 600°C. The heated piggery waste is then sent to a RYIELD reactor where all hydrogen was converted to H_2, all oxygen to O_2, all nitrogen to N_2, all sulfur to elementary S, and all carbon to elementary C. The product gas is then removed of all N_2 and S in the form of NH_3 and H_2S using a separator. This cleaned gas is then sent to a final RGIBBS reactor, where potential product species are set by those inputted to the model and calculated according to Gibbs energy minimisation. The species considered as products were H_2O, H_2, N_2, O_2, S, C, CO, CO_2, CH_4, H_2S, and NH_3.

All reactors within the MS-SCWG model were assumed to operate under isothermal and isobaric conditions without the use of catalysts. The heat streams for the RYIELD reactor and separator were fed to the RGIBBS reactor to determine the total heat duty of the SCWG reaction. From the MS-SCWG reactor, biogas with a 0.259 molar fraction CH_4, 0.212 molar fraction CO_2, and 0.068 molar fraction H_2 was produced.

3.2. Integrated Membrane Reactor

To perform the sequential modular simulation in Aspen Plus, it was assumed the reactor was operating under steady state, with counter current flow, constant pressure across the reactor, local equilibrium achieved in each partial area of the reactor, membrane is only selective to H_2, the CO content in the feed stream doesn't hinder the permeability of the membrane, all sweep steam entering the inlet of the reactor exits at the outlet, and there are no losses to reactor performance over time.

In the simulation, the separation of hydrogen gas through the membrane was split between n partial areas using a series of $(n+1)$ RGIBBS sub-reactors and n sub-separators. The RGIBBS sub-reactors model the local equilibrium reactions occurring across the MS-IMR as H_2 is permeated through the membrane and removed from the reactor by the sweep steam. After each sub-separator, which separates a permeated hydrogen stream from the feed

stream, the equilibrium for the WGS reaction in the feed stream is shifted to the left, the reactants side, as per Le Chatelier's principle, allowing the reaction to proceed further in favour of the products, H_2 and CO_2, until equilibrium is reached again between the reactants and products. Alternating the RGIBBS sub-reactors and the sub-separators, this H_2 removal and re-driving of the WGS reaction to equilibrium is modelled for each of the n partial areas of the MS-IMR and then summed to determine the final mole flow for the permeate and retentate streams. Each separated H_2 stream is combined in a mixer with the sweep steam stream to produce the final permeate stream product. After the nth sub-separator, the feed stream is sent to a final RGIBBS sub-reactor, from which the retentate CO_2, unreacted gases, and non-permeated H_2 exit the MS-IMR. Governing the membrane's permeance was the calculation of the hydrogen flux based off the hydrogen partial pressure difference between the feed side and permeate side of the membrane according to Sievert's law.

To calculate the hydrogen partial pressure difference, a 9.5 bar pressure on the feed side of the membrane, 0.4 bar pressure on the permeate side of the membrane, and 0.5 fraction of H_2 in the permeate stream (with the other 0.5 fraction H_2O from the permeated sweep steam) were used. The best case permeance of 15 $(Nm^3/h)/m^2/bar^{0.5}$ obtained from the membrane's characterisation was used. Providing the hydrogen flux in $(Nm^3/h)/m^2$, this calculation was then converted to flux on a mole basis, $(kmol/h)/m^2$, and multiplied by the area of the membrane to determine the total permeation of hydrogen. The area was calculated as that needed to remove 90% of H2 in the feed stream to the sub-separator,

$$Area = \frac{H2FEED \times 90\%}{H2FLUX} \tag{2}$$

based off the 90% recovery factor that was achieved by Giaconia et al. [1]. A steam to carbon ratio (s/c) (moles of H_2O to moles of atomic carbon) of 3.2mol/mol of sweep steam to feed stream was used, with the sweep steam entering the MS-IMR at 441°C. In their experimental work, Giaconia et al. found that methane conversion steadily increased with increasing s/c, achieving up to 99% conversion with a 13 mol/mol s/c with inlet molten salts at 544°C, but that only up to approximately 7 mol/mol did the s/c have a significant effect on the CH_4 conversion. Use of higher s/c were not recommended due to the higher heat input required for steam generation, leading to the optimal compromise of a 3.2 mol/mol s/c. The outlet retentate stream was assumed to exit at 8.5 bar and 590°C.

The ratio of H_2O to atomic carbon in the feed stream was also found to influence the H_2 permeation and CH_4 conversion in the MS-IMR. In the flowsheet, after exiting the MS-SCWG reactor and being cooled to 90°C, the liquefied water is removed from the product stream using a separator to be recycled or re-heated for use as sweep steam for the MS-IMR. The amount of H_2O in the feed stream to the MS-IMR can therefore be determined by the fraction of H_2O that is removed at this separator (H2OSEP). With no H_2O in the initial feed stream, the steam reforming reaction dominates over the WGS reaction, resulting in a higher yield of CO in the final retentate stream and reducing the mole fraction of CO_2. At higher mole flow rates of H_2O, the mole fraction of hydrogen in the feed stream is reduced, decreasing the hydrogen partial pressure difference between the feed and permeate side and thus the potential hydrogen that is permeated through the membrane. For the 10 partial areas, a H_2O mole flow in the feed stream was set for achieving a CH_4 conversion of 73% overall, as was achieved by Giaconia et al. The results of the sequential MS-IMR model was a plant output of 7.2 $kmolH_2/h$ (1,135 Nm^3/h of H_2) with a flow rate of 150 kg/h of dry piggery waste, a total membrane area of 131.8 m^2, 104.1 kW heat duty, and a 73% CH_4 conversion from the feed.

3.3. Sensitivity Analysis

Figure 3 shows the results of scenarios analysed to interpret the behaviour and sensitivity of the MS-SCWG reactor. Figure 3 (left) shows the effect of temperature of the MS-SCWG reactor, whereby the production of H_2 from the piggery waste is the most dependent on the reactor

temperature, significantly decreasing at temperatures below 550°C. Figure 3 (right) models the MS-SCWG reactor using five different ultimate and proximate analyses for the piggery waste [5], [19], [20], [21], showing how the product H_2 remains steady across all ultimate analyses but the product CH_4 and CO_2 experience significant variation, which could impact the results of the subsequent MS-IMR.

Figure 4 shows simulation results for the performance of the sequential model for the MS-IMR under different temperatures for the hot MS in the reactor's shell and for varying water mole fractions in the feed stream, which have been identified as two key parameters influencing the performance of the membrane. Figure 4 (left) shows that at higher MS temperature and with a higher water mole fraction in the feed stream, the flow rate of H_2 in the permeate increases. The results for the area of the membrane (Figure 4 (right)) are much more variable, specifically in the case of the 500°C MS where at low (below 0.3) and high (above 0.5) water mole fractions a very large area is needed to allow just a small permeation of H_2 or achieve a H_2 permeation close to that achieved at 550°C and 600°C. The two higher MS temperatures both follow similar trends for membrane area, with a minimum at 0.3 water mole fraction. For MS at 600°C, however, the area and H_2 permeation rate plateaus at water mole fractions >0.65 as the CH_4 in the stream reaches near to complete conversion, and the hydrogen partial pressure in the feed drops below the partial pressure in the permeate. Desirable operating ranges to reduce membrane area are therefore greater or equal to 550°C and at <0.5 water content.

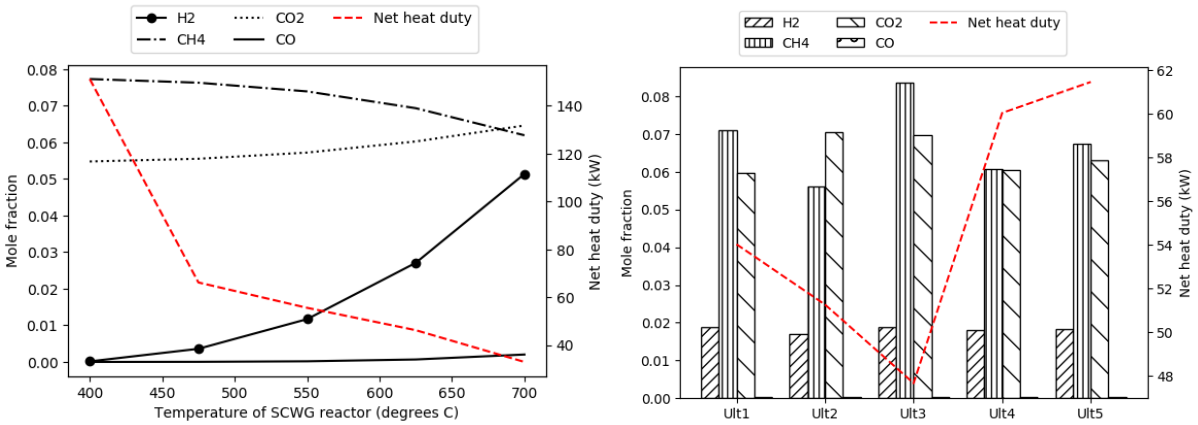

Figure 3. Effect of MS temperature and pig waste's ultimate analysis on MS-SCWG reactor.

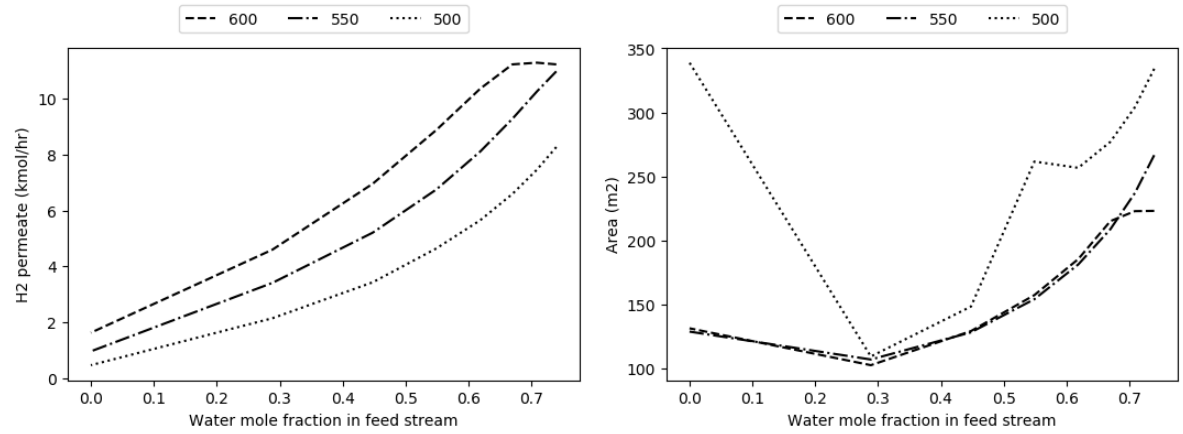

Figure 4. Total H_2 permeate flow rate and membrane area at different water mole fractions for IMR with MS at 600°C, 550°C, and 500°C.

4. Conclusion

The modelled technology of a system consisting of a 2.3 MWth CST plant with two tank molten salt (taken to be emerging 600°C solar salt) storage, an off-sun SCWG reactor, and a membrane reactor has achieved the production of a pure 7.2 kmol/h H_2 stream from 150 kg/h dry pig waste. From the MS-SCWG reactor, biogas with a 0.259 molar fraction of CH_4 was produced, which was then converted with a 73% efficiency in the MS-IMR using a membrane area of 131.8 m² and with a 63% pure CO_2 retentate stream. The proposed system has overcome barriers associated with on-sun SCWG/SMR, converting the piggery waste to H_2 within one integrated system and within the temperature bounds of molten salt, avoiding the high temperatures needed for conventional SMR. Going forward, optimisation of the system's exergy-based model, scale, and efficiency is needed, including the design of a more efficient heat exchanger network to reduce exergy losses throughout the system via coolers and other equipment. Improved designs should then be followed by a pilot project to test the system's performance against the mathematical and equilibrium-based model created in this work.

Data availability statement

All data used was taken from the literature and has been cited accordingly and can therefore be accessed via these references. This includes the piggery waste composition data and input parameters for the design of the MS-IMR.

Author contributions

Louise Bardwell: Methodology, Formal analysis, Writing – Original Draft **Alireza Rahbari:** Conceptualisation, Methodology, Supervision, Writing - Review & Editing **John Pye:** Conceptualisation, Methodology, Resources, and Supervision, Writing - Review & Editing

Competing interests

The ANU Centre for Entrepreneurial Agri-Technology (CEAT), who provided guidance and resources to the project, have received funding from Australian Pork Limited.

Acknowledgement

I would like to thank the Australian National University (ANU) Centre for Entrepreneurial Agri-Technology (CEAT) for the support and resources they have provided to the project, as well as my supervisors Dr John Pye and Dr Alireza Rahbari for all their time and support.

References

1. A. Giaconia, M. d. Falco, G. Caputo, R. Grena, P. Tarquini, and L. Marrelli, "Solar steam reforming of natural gas for hydrogen production using molten salt heat carriers," AIChE Journal, vol. 54, no. 7, pp. 1932–1944, 2008. doi: https://doi.org/10.1002/aic.11510.
2. IPCC, Ed., "Summary for Policymakers," in *Global Warming of 1.5°C: IPCC Special Report on Impacts of Global Warming of 1.5°C above Pre-industrial Levels in Context of Strengthening Response to Climate Change, Sustainable Development, and Efforts to Eradicate Poverty*, Cambridge: Cambridge University Press, 2022, pp. 1–24, doi: https://doi.org/10.1016/j.pecs.2017.04.001.
3. V. S. Sikarwar, M. Zhao, P. S. Fennell, N. Shah, and E. J. Anthony, "Progress in biofuel production from gasification," Progress in Energy and Combustion Science, vol. 61, pp. 189–248, Jul. 2017, doi: https://doi.org/10.1016/j.pecs.2017.04.001.

4. A. Bonk, M. Braun, A. Hanke, V.A. Sötz, T. Bauer, AIP Conference Proceedings 2303 (2020) 190003.
5. A. Rahbari, A. Shirazi, and J. Pye, “Methanol fuel production from solar-assisted supercritical water gasification of algae: a techno-economic annual optimisation,” *Sustainable Energy Fuels*, vol. 5, no. 19, pp. 4913–4931, Sep. 2021.
6. A. Rahbari, M. B. Venkataraman, and J. Pye, “Energy and exergy analysis of concentrated solar supercritical water gasification of algal biomass,” *Applied Energy*, vol. 228, pp. 1669–1682, Oct. 2018, doi: https://doi.org/10.1016/j.apenergy.2018.07.002.
7. A. Rahbari, A. Shirazi, M. B. Venkataraman, and J. Pye, “A solar fuel plant via supercritical water gasification integrated with Fischer–Tropsch synthesis: Steady-state modelling and techno-economic assessment,” *Energy Conversion and Management*, vol. 184, pp. 636–648, Mar. 2019, doi: https://doi.org/10.1016/j.enconman.2019.01.033.
8. A. Shirazi, A. Rahbari, C.-A. Asselineau, and J. Pye, “A solar fuel plant via supercritical water gasification integrated with Fischer–Tropsch synthesis: System-level dynamic simulation and optimisation,” *Energy Conversion and Management*, vol. 192, pp. 71–87, Jul. 2019, doi: https://doi.org/10.1016/j.enconman.2019.04.008.
9. A. Rahbari, A. Shirazi, M. B. Venkataraman, and J. Pye, “Solar fuels from supercritical water gasification of algae: Impacts of low-cost hydrogen on reformer configurations,” *Applied Energy*, vol. 288, p. 116620, Apr. 2021, doi: https://doi.org/10.1016/j.apenergy.2021.116620.
10. M. B. Venkataraman, A. Rahbari, P. van Eyk, A. W. Weimer, W. Lipiński, and J. Pye, “Liquid fuel production via supercritical water gasification of algae: a role for solar heat integration?,” *Sustainable Energy Fuels*, vol. 5, no. 24, pp. 6269–6297, Dec. 2021, doi: https://doi.org/10.1039/D1SE01615F.
11. A. Giaconia, G. Iaquaniello, G. Caputo, B. Morico, A. Salladini, L. Turchetti, G. Monteleone, A. Giannini, and E. Palo, “Experimental validation of a pilot membrane reactor for hydrogen production by solar steam reforming of methane at maximum 550 °C using molten salts as heat transfer fluid,” International Journal of Hydrogen Energy, vol. 45, no. 58, pp. 33 088–33 101, Nov. 2020, doi: https://doi.org/10.1016/j.ijhydene.2020.09.070.
12. F.A.O. of the United Nations, “Global Livestock Environmental Assessment Model (GLEAM),” 2020.
13. Australian Government, “Animal effluent management method,” 2021.
14. M. Sharara and S. Sadaka, “Thermogravimetric Analysis of Swine Manure Solids Obtained from Farrowing, and Growing-Finishing Farms,” Journal of Sustainable Bioenergy Systems, vol. 4, no. 1, pp. 75–86, Mar. 2014, number: 1 Publisher: Scientific Research Publishing, doi: https://doi.org/10.4236/jsbs.2014.41008.
15. W.-D. Steinmann, “Thermal energy storage systems for concentrating solar power (csp) plants,” in Concentrating solar power technology: Principles, developments and applications. Woodhead Publishing Limited, pp. 16–25.
16. D. Castello and L. Fiori, “Supercritical water gasification of biomass: Thermodynamic constraints,” Bioresource Technology, vol. 102, no. 16, pp. 7574–7582, Aug. 2011, doi: https://doi.org/10.1016/j.biortech.2011.05.017.
17. O. Yakaboylu, J. Harinck, K. G. Gerton Smit, and W. de Jong, “Supercritical water gasification of manure: A thermodynamic equilibrium modeling approach,” Biomass and Bioenergy, vol. 59, pp. 253–263, Dec. 2013, doi: https://doi.org/10.1016/j.biombioe.2013.07.011.
18. N. A. Al-Mufachi, N. V. Rees, and R. Steinberger-Wilkens, “Hydrogen selective membranes: A review of palladium-based dense metal membranes,” Renewable and Sustainable Energy Reviews, vol. 47, pp. 540–551, Jul. 2015, doi: 10.1016/j.rser.2015.03.026.
19. Biofuels Research Infrastructure (BRISK). “Phyllis2.” https://phyllis.nl/ (Sep. 2021)
20. S. M. Heilmann *et al.*, “Phosphorus Reclamation through Hydrothermal Carbonization of Animal Manures,” *Environ. Sci. Technol.*, vol. 48, no. 17, pp. 10323–10329, Sep. 2014, doi: https://doi.org/10.1021/es501872k.
21. X. Cao, K. S. Ro, M. Chappell, Y. Li, and J. Mao, “Chemical Structures of Swine-Manure Chars Produced under Different Carbonization Conditions Investigated by Advanced

Solid-State 13C Nuclear Magnetic Resonance (NMR) Spectroscopy," *Energy Fuels*, vol. 25, no. 1, pp. 388–397, Jan. 2011, doi: https://doi.org/10.1021/ef101342v.